THE APPLICATION OF THE PHASE SPACE TIME EVOLUTION METHOD TO ELECTRON SHIELDING*

Matthew C. Cordaro, Long Island Lighting Company

and

Martin S. Zucker, Brookhaven National Laboratory

A computer-based method for treating the motion of charged and neutral particles called the Phase Space Time Evolution method (PSTE) has been developed. This technique, instead of utilizing the integro-differential transport equation and solving it by computer methods, makes direct use of the computer by employing its bookkeeping capacity to literally keep track of the time development of a phase space distribution of particles. This method is applied in this paper to a study of the penetration of electrons. In this application use is made of the continuous slowing down approximation for energy degradation and the Goudsmit-Saunderson distribution for multiple scattering. The specific problem investigated considers a 1 MeV beam of electrons normally incident on a semi-infinite slab of aluminum. Results of the PSTE calculation for this problem are compared on the basis of number transmission, energy spectrum and angular distribution as a function of penetration with existing Monte Carlo calculations and experimental results. The general agreement exhibited is good. In addition to the above, time-dependent PSTE electron penetration results for the same problem are presented. The computer time required to make the PSTE calculation discussed here was approximately 10 minutes on the CDC 6600 computer at the Brookhaven National Laboratory. This can be compared to a Monte Carlo calculation on a similar machine which requires on the order of an hour or more of computer time. As an added feature, the PSTE method generates deterministic and time dependent results during the small amount of machine time it requires.

SYMBOL MEANINGS

E	Energy
X	Position
μ_x	Cosine of the polar angle with respect to the X direction
t	Time
Δt	Time interval
v	Speed
S	Pathlength
Z	Atomic number
c	Speed of light
$m_o c^2$	Rest mass energy
ΔS_x	X displacement
ΔE	Energy interval
F	Apportioning fraction
ΔX	Position interval
ρ	Particle density
μ_i	Cosine of the polar angle of incidence with respect to the X direction
$p(\mu_x \mid \mu_i)$	Angular probability density function with respect to μ_x given an incident direction μ_i independent of incident and scattered azimuthal angle
$P_\ell(\mu)$	Legendre Polynomial of index ℓ
$G_\ell(S)$	Goudsmit-Saunderson distribution expansion terms
N	Number of scatterers per unit volume
θ_s	Polar angle of scattering relative to an arbitrary incident direction

*This work was performed under the auspices of the United States Atomic Energy Commission.

SYMBOL MEANINGS
(continued)

$\sigma(\theta_s,S)$	Coulomb single scattering cross section
$T_N(x)$	Number transmission factor
$\Delta\mu_x$	Cosine interval
$J(X,E,\mu_x,t)$	Current
E_i	Initial or incident energy
$T_N(X,E)$	Function representing energy spectrum
$T_N(X,\mu_x)$	Function representing angular distribution
$J_{X_+}(X,t)$	Transmitted current

INTRODUCTION

When traversing even a thin layer of matter, electrons engage in numerous collisions which produce in most cases small energy losses and deflections. In addition, they may undergo a relatively small number of catastrophic collisions which cause them to lose an appreciable fraction of their energy and to scatter through a large angle. The combined effect of all collisions is a complex transport process which requires an elaborate theory for description.

Monte Carlo methods of calculation have been applied to electron shielding calculations and in fact have been considered up to now the most accurate available, even though significant limitations are recognized. As with other Monte Carlo based calculations, the answers obtained can only be known with an accuracy which is governed by the statistical uncertainty inherent in the stochastic nature of the Monte Carlo method. Since individual electron slowing down case histories can be extremely complex, enormous amounts of computer time may be required to generate a statistically representative number of individual histories. This is the case even with the application of special techniques adapting Monte Carlo to the requirements of electron slowing down. Another problem with the Monte Carlo approach is that it seems suitable for handling only steady state or time independent phenomena; at least the present authors are unaware of any charged particle Monte Carlo calculations structured to take into account time dependence.

A computer-based method of treating the motion of charged or neutral particles which overcomes these difficulties has been introduced by Tavel and Zucker [1,2,3,4]. This technique, referred to as the "Phase Space Time Evolution" (PSTE) method, has been successful in the several neutron transport problems it has thus far been applied to [4]. The present paper will deal with the first application of the PSTE method to a charged particle problem, namely, electron slowing down and shielding in a semi-infinite medium.

The classical analytical approach to transport calculations usually requires the solving of an integro-differential equation subject to boundary conditions established by the problem of interest. The equation itself is a mathematical representation of the space-time evolution of a particle distribution which has been derived from the application of continuity principles in phase space. Instead of utilizing an integro-differential equation and solving it by computer techniques, the PSTE method makes direct use of the computer and employs its bookkeeping capacity to literally keep track of the time development of the phase space distribution.

The PSTE method was extended significantly beyond the approach used for neutron problems detailed in reference 4 in order to investigate the transport of electrons. This involved the addition of energy as a third dimension of the phase space and the use of multiple interaction theories for particle transport.

Defining the Three-Dimensional Digitized Phase Space

The phase space within which the flight of electrons can be traced which is shown in Figure 1 has Cartesian axes representing energy, E, position, X and cosine of the polar angle with respect to the X axis, μ_x. The values of E range from the maximum energy considered in the problem at the origin to the lowest energy of interest. The values of X can vary between any desired one dimensional spatial limit. The direction cosine, μ_x, ranges from +1 to -1.

The particle density in the phase space is stored as the number of particles per unit length in the element of phase space between coordinates X_{i-1} and X_i with energy E_K and direction cosine μ_{x_j}.

SOLVING A PROBLEM

An initial particle distribution represents the state of the phase space at time zero. The time iterative scheme used in the calculation then traces the movement of each element of phase space for one time interval Δt. As illustrated in Figure 2 during this time interval the element of phase space is first relocated in the E-X plane.

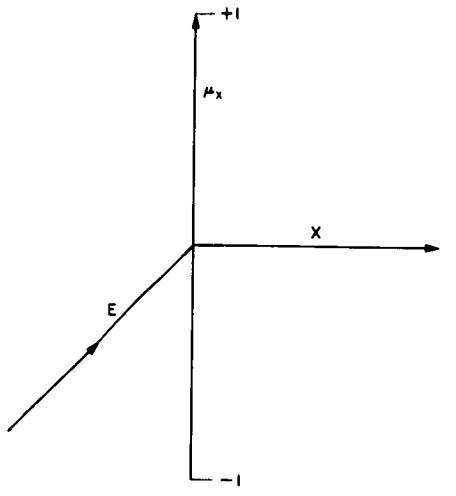

Figure 1 An illustration of the three dimensional phase space.

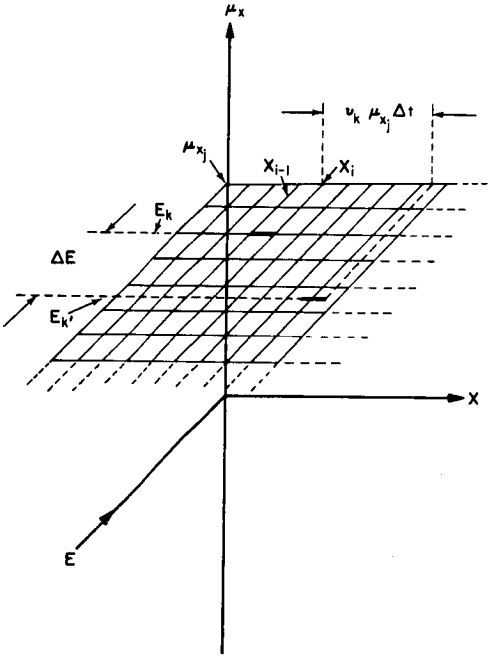

Figure 2 Movement of an element of phase space in the E-X plane.

In the calculations presented in this paper continuous slowing down theory as formulated by Rohrlich and Carlson [5], has been used to determine the energy loss of an element during Δt. Therefore, if the particles represented by an element of phase space are assumed to be traveling at an initial speed, v_K, corresponding to their initial kinetic energy, E_k, after a small time interval, Δt, their final kinetic energy, E_K', is approximately given by

$$E_K' = E_k - |dE_k/dS| v_k \Delta t \qquad (1)$$

where

$$v_k = c\left(1 - [m_o c^2/(E_k+m_o c^2)]^2\right)^{\frac{1}{2}} \qquad (2)$$

and $|dE_k/dS|$ is the stopping power given in reference 5. By using the fact that the radiative contribution to slowing down is approximately given by [6]

$$-dE_k/dS \ (ZE_k/800), \ ZE_k << 800$$

where $-dE_k/dS$ is the energy loss per unit pathlength due to nonradiative collisions, the energy loss from radiative collisions has been included in eq. (1) by multiplying $|dE_k/dS|$ by the factor $[1+ZE_k/800]$. It should be mentioned here that the PSTE method does not require the use of continuous slowing down. Straggling (energy loss fluctuations) can also be handled within the framework of this method. It was intended, however, in the present application to first see how well the method performed without this complication, which has been left for future work,

The technique employed to take into account the functional dependence on energy of dE/dS and v in eq. 1 divides the time interval Δt into many smaller intervals during which it is assumed that dE/dS and v remain constant. After each time increment the resulting final energy, E_k', calculated is used to establish the values of dE/dS and v to be used for the next smaller time step. The total pathlength traveled during Δt and the final energy after Δt are obtained by adding the contributions of all the smaller time steps.

In addition to providing the total pathlength traveled and the final energy, the iterative procedure outlined for eq. (1) also generates an average speed $\bar{v}_k$ for the time interval Δt. Once this value is available the displacement of the phase space element can be found through use of the relation

$$\Delta S_x = \bar{v}_k \mu_{x_j} \Delta t \qquad (3)$$

where μ_{x_j} is the initial direction cosine of the element and ΔS_x is its displacement after Δt. Once the X displacement has been determined the new position of the element X' is given by

$$X' = X + \Delta S_x. \qquad (4)$$

An important assumption in the determination of the X displacement is that μ_{x_j} does not change appreciably during Δt. This approximation is very good for small values of Δt. A constant μ_{x_j} during Δt is assumed mainly to avoid excessive computer time which contributes little to the accuracy of the electron PSTE calculation.

After an element of phase space has been moved in the E-X plane, it must be apportioned to the established grid lines (digitized). A moments weighting technique is used by the application presented in this paper to carry out the apportionment in energy.

The procedure followed first establishes the difference between the final energy and the end points of the energy grid interval into which the phase space element being operated upon falls. Thus, if some final energy of an element, E', falls between $E_{k'-1}$ and $E_{k'}$, these differences are $E_{k'-1} - E'$ and $E' - E_{k'}$, respectively. Once these values are found they are divided by ΔE, the energy interval between grid lines, to establish the energy apportioning fractions (moments),

$$F_{k'} = \frac{E_{k'-1} - E'}{\Delta E} \tag{5}$$

and

$$F_{K'-1} = \frac{E' - E_{k'}}{\Delta E} \quad . \tag{6}$$

A similar procedure is involved in digitizing the final position coordinate. Suppose that the original element intersects the grid line $X_{i'}$ with its end points falling on some $X_1 < X_{i'}$ and $X_2 > X_{i'}$ respectively. Then the distance $X_{i'} - X_1$ and $X_2 - X_{i'}$, divided by the increment of distance between grid lines, ΔX, are the position apportioning fractions,

$$F_{i'} = \frac{X_{i'} - X_1}{\Delta X} \tag{7}$$

and

$$F_{i'+1} = \frac{X_2 - X_{i'}}{\Delta X} \quad . \tag{8}$$

The four fractions, $F_{k'-1}$, and $F_{k'}$ representing energy apportionment and $F_{i'}$ and $F_{i'+1}$ representing spatial distribution, determine the digitization or apportionment in the E-X plane. Therefore, the number of particles per unit length contributed by the transported element having an initial particle density of $\rho_{k,j,i}$ (neglecting for the moment angular dependence)

at $E_{k'-1}$, μ_{x_j} between $X_{i'-1}$ and $X_{i'}$ is

$$\rho_{k'-1,j,i'} = \rho_{k,j,i} [F_{k'-1} F_{i'}];$$

at $E_{k'-1}$, μ_{x_j} between $X_{i'}$ and $X_{i'+1}$ is

$$\rho_{k'-1,j,i'-1} = \rho_{k,j,i} [F_{k'-1} F_{i'+1}];$$

at $E_{k'}$, μ_{x_j} between $X_{i'-1}$ and $X_{i'}$ is

$$\rho_{k',j,i'} = \rho_{k,j,i} [F_{k'} F_{i'}];$$ and

at $E_{k'}$, μ_{x_j} between $X_{i'}$ and $X_{i'+1}$ is

$$\rho_{k',j,i'+1} = \rho_{k,j,i} [F_{k'} F_{i'+1}].$$

The only operation remaining to complete the movement of the original element for Δt is its distribution in μ_x. To perform this operation the Goudsmit-Saunderson distribution [7,8] for multiple scattering was modified to provide the angular distribution of scattering referenced to the X direction independent of azimuthal angle,

$$p(\mu_x|\mu_i) = \sum_{\ell=0}^{\infty} \frac{2\ell+1}{2} \exp\left[-\int_0^s G_\ell(s')ds'\right] P_\ell(\mu_i) P_\ell(\mu_x) \tag{9}$$

where

$$G_\ell(s) = 2\pi N \int_0^\pi \sigma(\theta_s, S) \left[1 - P_\ell(\cos\theta_s)\right] \sin\theta_s d\theta_s \tag{10}$$

and μ_x and μ_i are the cosines of the polar angles of scattering and incidence, respectively, referenced to the X direction. To utilize the modified angular distribution in the PSTE calculation, the probability density given in eq. (9) is evaluated in the following way. First the interval $-1 \le \mu_x \le 1$ is divided into subintervals in such a manner that a grid line lies in the middle of each interval. The probability, therefore, of obtaining some $\mu_{x'}$ in the interval $\mu_b \le \mu_x \le \mu_a$ is given by

$$\int_{\mu_b}^{\mu_a} p(\mu_x|\mu_i) d\mu_x = \tfrac{1}{2}(\mu_a - \mu_b)$$

$$+\tfrac{1}{2}\sum_{\ell=1}^{\infty}\exp\left[\int_0^s G_\ell(s')ds'\right]P_\ell(\mu_i)$$
$$\left\{\left[P_{\ell+1}(\mu_a)-P_{\ell-1}(\mu_a)\right]\right.$$
$$\left.+\left[P_{\ell-1}(\mu_b)-P_{\ell+1}(\mu_b)\right]\right\}. \qquad (11)$$

Eq. (11) is applied to all subintervals. The probabilities generated in turn serve as weighting functions for the apportionment of the original transported element in μ_x.

Once every element in the phase space has been operated upon as outlined above, the stored results are tested against a set of terminating criteria for the problem being investigated. If these criteria are satisfied the calculation is completed. If not, another iteration is required. The final result of the PSTE calculation is a complete record of the time evolution of a particle density distribution given as a function of energy, direction and position.

Comparison of PSTE Calculations with Electron Monte Carlo and Experimental Results

To assess the validity of the results provided by the PSTE method as applied to electron transport, a comparison was made with Monte Carlo calculations and experimental results for a shielding problem which considered a 1 MeV pulse of electrons normally incident on a semi-infinite slab of aluminum. Comparisons were made on the basis of the different forms of published Monte Carlo and experimental results for this problem.

The first form of result compared is the number transmission factor. This factor, $T_N(X)$, which provides the fraction of incident electrons transmitted past X, is defined by

$$T_N(X) = \frac{1}{\Delta E\Delta\mu_x}\int_0^{E_i}\int_0^{1}\int_0^{t} J(X,E,\mu_x,t')dt'd\mu_x dE \qquad (12)$$

where the current $J(X,E,\mu_x,t)$ is given by

$$J(X,E,\mu_x,t) = \rho(X,E,\mu_x,t)v(E)\mu_x, \qquad (13)$$

E_i is the incident energy of the electrons and t is the time required for the entire pulse to essentially pass through the medium. Comparison of the PSTE generated number transmission curve with several Monte Carlo and experimental results is given in Figure 3. Penetration (X) in this case is represented as the fraction of the mean range traversed. The Monte Carlo results include calculations by Berger [9,10, 11] which use continuous slowing down in one case and straggling (energy loss fluctuation) in the other. Also shown are Monte Carlo calculations made by Perkins [12] which include the effects of straggling. The experimental points depicted include the results of experiments conducted by Rester [13] for 1 MeV electrons. Since the number transmission curve plotted as a function of the mean range traversed is approximately independent of initial energy in the neighborhood of 1 MeV, the average results of Agu et al. [14] for experiments conducted at energies below 1 MeV have also been used for comparison purposes. The agreement exhibited in Figure 3 between the PSTE and the Monte Carlo and experimental results is good. The PSTE curve, as should be expected, falls below the Monte Carlo and experimental results which considered straggling effects since, as mentioned before, this PSTE calculation utilized the continuous slowing down approximation for energy degradation. Although the experimental points of Rester lie somewhat above the PSTE curve, it should be noted that the PSTE values fall within the range of experimental uncertainty associated with these results.

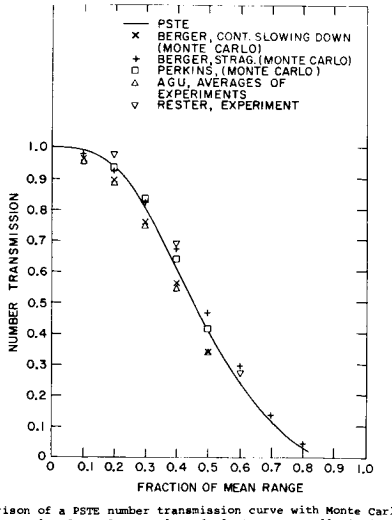

Figure 3 Comparison of a PSTE number transmission curve with Monte Carlo and experimental results for a 1 MeV pulse of electrons normally incident on a semi-infinite slad of aluminum.

The energy spectrum of transmitted electrons produced by the PSTE calculation for the problem under consideration is a critical indication of agreement with existing calculations and experimental results. The energy spectrum $T_N(X,E)$ is related to the PSTE generated current by

$$T_N(X,E) = \frac{1}{\Delta E \Delta \mu_x} \int_0^1 \int_0^t J(X,E,\mu_x,t')dt'd\mu_x \quad . \qquad (14)$$

The shapes of PSTE energy spectra for three different penetrations in terms of fractions of the mean range are compared to Monte Carlo and experimental results documented by Rester [13] in Figures 4 - 6. The Monte Carlo calculations were performed by Berger. Assuming that the total number of particles present at each penetration investigated is approximately the same for the PSTE, Monte Carlo and experimental examples, the histograms in Figures 4 - 6 have been drawn on a scale relative to the maximum of each distribution. In this way it is possible to separate an examination of the energy spectrum from other considerations. In other words, it is only intended here to investigate the relative

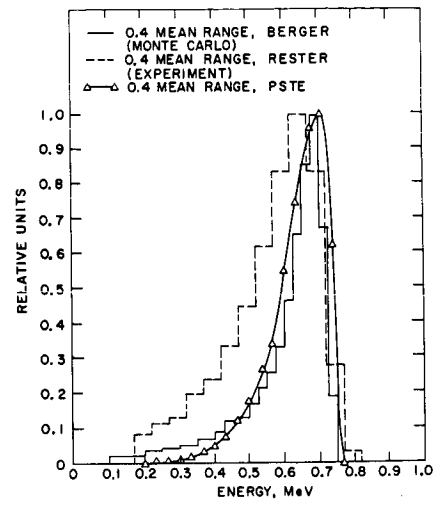

Figure 5 Comparison of the PSTE transmitted energy spectrum with Monte Carlo and experimental results at approximately .4 mean range for a 1 MeV pulse of electrons normally incident on a semi-infinite slab of aluminum.

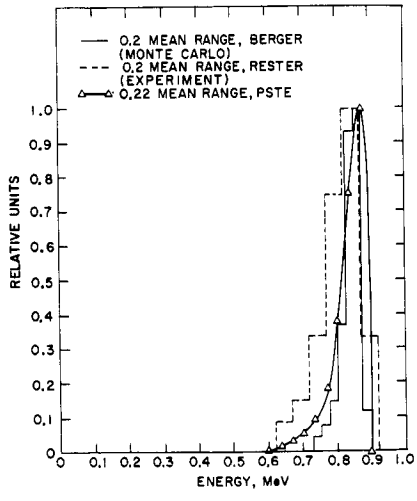

Figure 4 Comparison of the PSTE transmitted energy spectrum with Monte Carlo and experimental results at approximately .2 mean range for a 1 MeV pulse of electrons normally incident on a semi-infinite slab of aluminum.

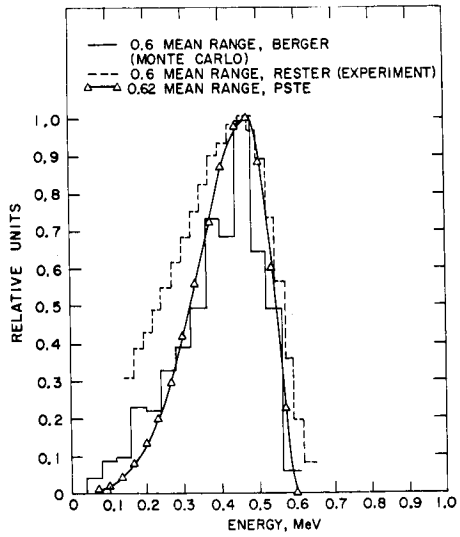

Figure 6 Comparison of the PSTE transmitted energy spectrum with Monte Carlo and experimental results at approximately .6 mean range for a 1 MeV pulse of electrons normally incident on a semi-infinite slab of aluminum.

shapes of the different energy spectra and not the total number of particles at a specific penetration (this has been done in the consideration of the number transmission factor). The good general agreement between Monte Carlo and experimental results and the PSTE calculation is well illustrated in Figures 4 - 6. For each penetration the PSTE result agrees very well with the Monte Carlo histogram. The agreement is not as good when the PSTE results are compared to the experimental values. The largest discrepancy appears at .4 of the mean range where the disparity between the Monte Carlo and experimental results is the greatest.

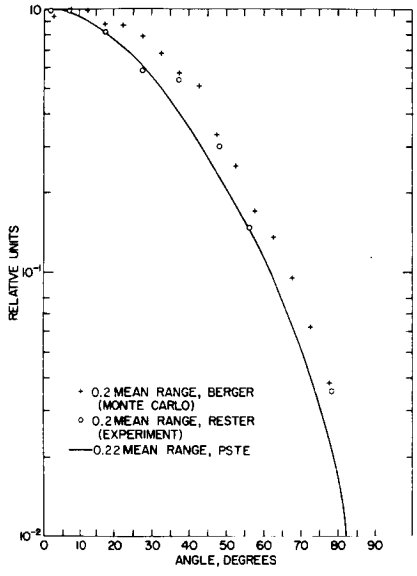

Figure 7 Comparison of the PSTE transmitted angular distribution with Monte Carlo and experimental results at approximately .2 mean range for a 1 MeV pulse of electrons normally incident on a semi-infinite slab of aluminum.

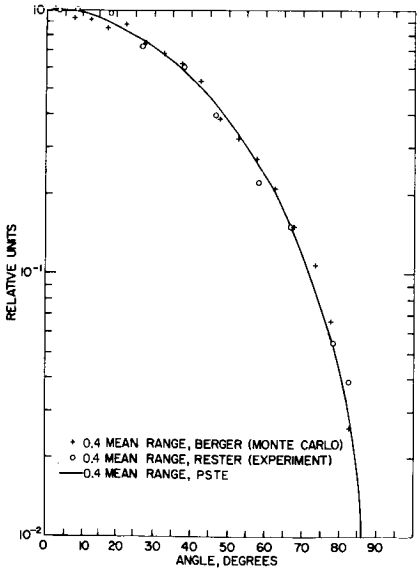

Figure 8 Comparison of the PSTE transmitted angular distribution with Monte Carlo and experimental results at approximately .4 mean range for a 1 MeV pulse of electrons normally incident on a semi-infinite slab of aluminum.

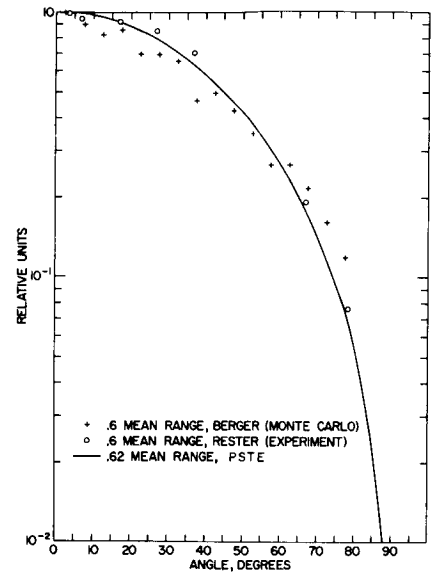

Figure 9 Comparison of the PSTE transmitted angular distribution with Monte Carlo and experimental results at approximately .6 mean range for a 1 MeV pulse of electrons normally incident on a semi-infinite slab of aluminum.

The angular distribution of transmitted electrons produced by the PSTE calculation has also been compared to Monte Carlo and experimental results. The angular distribution $T_N(X,\mu_X)$ is defined by

$$T_N(X,\mu_X) = \frac{1}{\Delta E \Delta \mu_X} \int_0^{E_i} \int_0^{t} J(X,E,\mu_X,t')dt'dE \qquad (15)$$

where $0 \leq \mu_X \leq 1$. The shapes of the angular distribution curves for the same three penetrations used in the energy spectrum investigation are compared in Figures 7 - 9. Again the curves are drawn on a scale relative to the maximum of each distribution for the same reasons outlined in the discussion of the energy spectrum. The results used for comparison are Monte Carlo calculations made by Berger and experiments conducted by Rester, the data for both being taken from publications authored by Rester [13,15]. In general there is acceptable agreement between the PSTE results and the Monte Carlo and experimental points. For all three penetrations the PSTE curve agrees very well with the experimental values. The largest discrepancy between the PSTE and Monte Carlo results occurs at the smallest and largest penetrations considered. Interestingly the greatest difference between the Monte Carlo and experimental values also occurs at these depths.

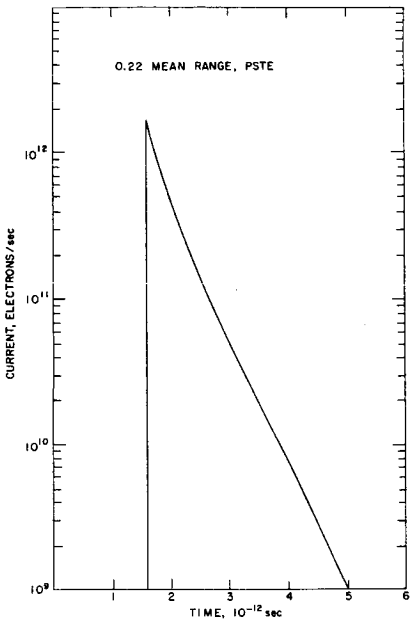

Figure 10 Transmitted current at 0.22 mean range for a 1 MeV pulse of electrons normally incident on a semi-infinite slab of aluminum resulting in an incident current of about 3.2×10^{12} electrons per second.

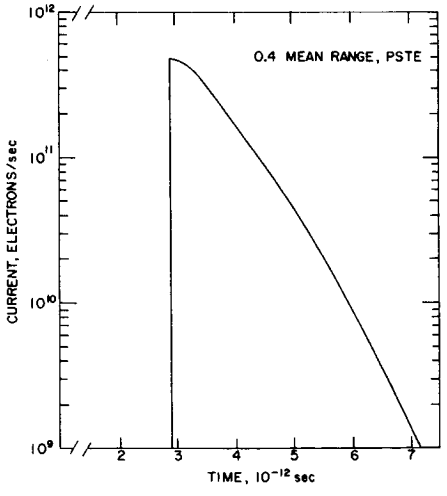

Figure 11 Transmitted current at 0.4 mean range for a 1 MeV pulse of electrons normally incident on a semi-infinite slab of aluminum resulting in an incident current of about 3.2×10^{12} electrons per second.

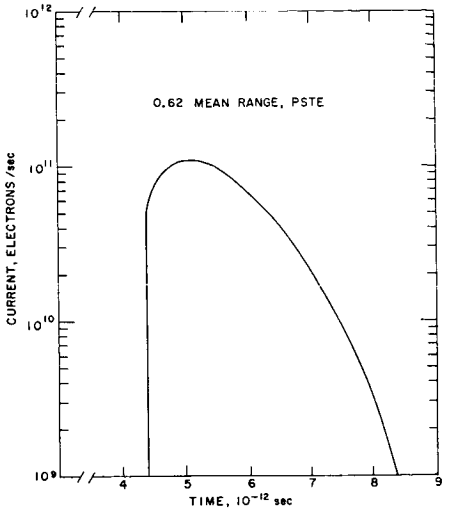

Figure 12 Transmitted current at 0.62 mean range for a 1 MeV pulse of electrons normally incident on a semi-infinite slab of aluminum resulting in an incident current of about 3.2×10^{12} electrons per second.

Time Dependent Results

One of the more significant contributions of the PSTE method is the time dependent results it provides. In Figures 10 - 12 plots of the time dependent transmitted current $J_{x_+}(X,t)$ given by

$$J_{x_+}(X,t) = \frac{1}{\Delta E \Delta \mu_x} \int_0^{E_i} \int_0^1 J(X,E,\mu_x,t) d\mu_x dE \qquad (16)$$

for the problem in question are presented. The penetrations considered are the same as those examined for the energy spectrum and angular distribution. At the small penetration (.22 mean range) the transmitted current reaches a maxmum very quickly and then decreases rapidly with time. The intermediate penetration (.4 mean range) results exhibit much of the same behavior but the current drops off at a slower rate as time increases. At the largest penetration (.62 mean range) there is a more gradual build-up to the maximum transmitted current achieved and a less rapid decrease with time than at the other penetrations. This is probably because at this depth the electrons are diffusing through medium and are characterized by relatively broad energy spectra and angular distributions.

Another way of looking at the time dependent results provided by the PSTE method is illustrated in Figure 13. Here the current as a function of position with time as a parameter has been traced by the computer. The time interval between plotted iterations is approximately 3.2×10^{-13} seconds. Essentially this figure represents a picture of the time evolution of the transmitted current in the aluminum slab. At first the current builds up rapidly and declines rapidly as the electrons enter the medium. There is also a significant reduction in the maximum transmitted current from one iteration to the other. At larger penetrations or at a later time, however, the curves representing the distribution of the transmitted current as a function of penetration become broader. This is understandable due to the fact that at later points in time the electrons are diffusing through the medium and have broad energy spectra and angular distributions. This parallels the reasoning used to describe the shape of the transmitted current curve as a function of time at the largest penetration examined (.62 mean range, Figure 12).

Advantages of the PSTE Method

One of the most attractive features of the PSTE method is the comparatively small amount of computer time it requires. For example, the PSTE calculations discussed in this paper required approximately ten minutes of computer time on the CDC 6600 computer at the Brookhaven National Laboratory. This compares to a Monte Carlo calculation for the same problem which requires on the order of an hour or more of computer time.

Another advantage of the PSTE method is that it provides deterministic results. This can be contrasted to the results of a Monte Carlo calculation which have a statiscal uncertainty associated with them dependent on the number of histories sampled.

Finally, the PSTE method generates a complete record of the time evolution of a particle density distribution. As stated previously, the authors are unaware of any successful Monte Carlo attempts at providing time dependent results for charged particle problems. It is the authors' opinion that the PSTE method is ideally suited for this application.

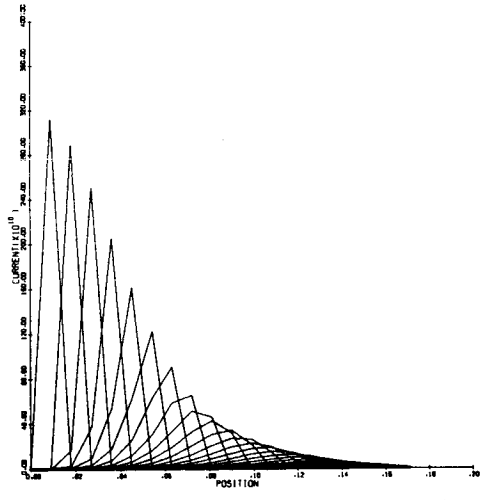

Figure 13 Time evolution of transmitted current for a 1 MeV pulse of electrons normally incident on a semi-infinite slab of aluminum resulting in an incident current of about 3.2×10^{12} electrons per second.

Acknowledgement

The material presented in this paper represents part of a thesis submitted by M. C. Cordaro in partial fulfillment of the requirements for the degree of Doctor of Philosophy at the Cooper Union. The authors wish to express their appreciation to Dr. Richard Felder for supplying a computer program to evaluate the Goudsmit-Saunderson distribution.

References

1. Tavel, M. A. and Zucker, M. S., "A Method of Solving Time-Dependent Transport Problems," Trans. Amer. Nucl. Soc. 10, 213 (1967).

2. Tavel, M. A. and Zucker, M. S., "Improvements on a New Method for Time-Dependent Neutron Problems," Trans. Amer. Nucl. Soc. 11, 557 (1968).

3. Tavel, M. A. and Zucker, M. S., "Some Quantitative Results and New Application of the Phase-Space Time Evolution Method," Trans. Amer. Nucl. Soc. 12, 158 (1969).

4. Tavel, M. A. and Zucker, M. S., "The Phase Space Time Evolution Method," Transport Theory and Statistical Physics 1, (in press).

5. Rohrlich, F. and Carlson, B. C., "Positron - Electron Differences in Energy Loss and Multiple Scattering," Phys. Rev. 93, 38 (1954).

6. Fitzgerald, J. J., Brownell, G. L., and Mahoney, F. J., Mathematical Theory of Radiation Dosimetry, Gorden and Breach, New York, 1967.

7. Goudsmit, S. and Saunderson, J. L., "Multiple Scattering of Electrons," Phys. Rev. 58, 36, (1950).

8. Goudsmit, S. and Saunderson, J. L., "Multiple Scattering of Electrons, II," Phys. Rev. 58, 36 (1940).

9. Berger, M. J., Transmission and Reflection of Electrons by Aluminum Foils, NBS Tech. Note 187, National Bureau of Standards, 1963.

10. Berger, M. J. and Seltzer, S. M., "Results of Some Recent Transport Calculations for Electrons and Bremsstrahlung," p. 437, NASA SP-71, National Aeronautics and Space Administration, 1964.

11. Berger, M. J. and Seltzer, S. M., Transmission of 1-MeV Electrons Through Aluminum, NBS 8900, National Bureau of Standards, 1965.

12. Perkins, J. F., "Monte Carlo Calculation of Transport of Fast Electrons," Phys. Rev. 126, 1781 (1962).

13. Rester, D. H. and Dance, W. E., Electron Scattering and Bremsstrahlung Measurements, NASA CR-759, National Aeornautics and Space Administration, 1967.

14. Agu, N. C., Burdett T., and Matsukawa, E., "Transmission of Electrons through Aluminum Foils," Proc. Soc. London 71, 201 (1958).

15. Rester, D. H. and Rainwater, W. J., "Coulomb Scattering of Electrons in Aluminum Without Atomic Excitation," Phys. Rev. 140, A165 (1956).

16. Cordaro, M. C. and Zucker, M. S., "A Method for Solving Time-Dependent Electron Transport Problems" Trans. Amer. Nucl. Soc. 13, 630 (1970).

17. Tavel, M. A. and Zucker, M. S., "The Phase Space Time Evolution Method, etc.," Trans. Amer. Nucl. Soc. 13, 695 (1970).